Supporting Information

Trimetallic-Organic Framework/ MXene Composite as an Oxygen Evolution Reaction Electrocatalyst with Elevated Intrinsic Activity

Mahrokh Nazari[†], Ali Morsali[†]*

[†]Department of Chemistry, Faculty of Basic Sciences, Tarbiat Modares University, Tehran 14117-13116, P.O. Box 14115-175, Iran;https://orcid.org/0000-0002-1828-7287

Email: morsali_a@modares.ac.ir

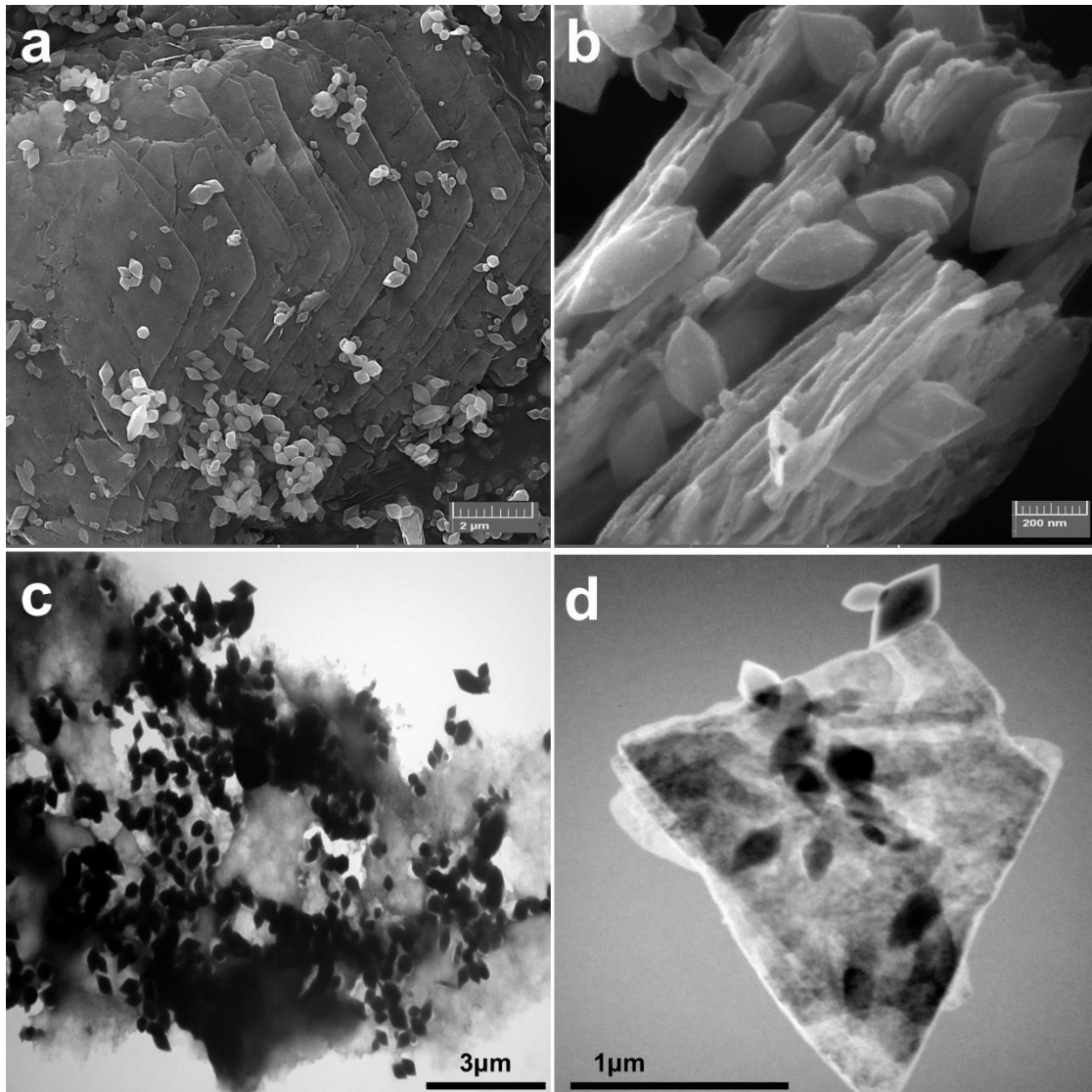## 1. FESEM and TEM images of FeNiCo-MIL/Ti$_3$C$_2$ composite

Figure S 1. *(a and b) FESEM image of FeNiCo-MIL/Ti$_3$C$_2$ composite from top and side view, (c and d) TEM and dark field TEM images of FeNiCo-MIL/Ti$_3$C$_2$ in different magnifications respectively.*
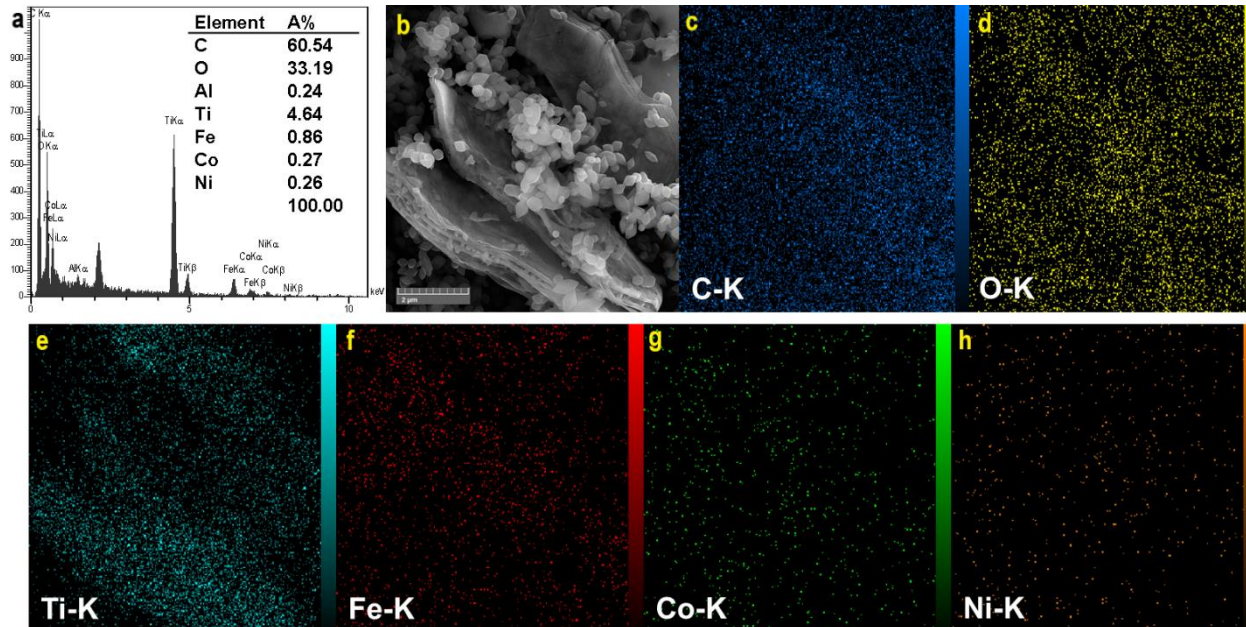
2. EDX and elemental mapping

Figure S 2. EDS spectrum and elemental mapping of FeNiCo-MIL/Ti₃C₂ composite. *(a) EDS spectrum of the FeNiCo-MIL/Ti₃C₂ composite, (b) FE-SEM image and (c-) EDS elemental mappings of carbon, oxygen, titanium, iron, cobalt and nickel elements of the FeNiCo-MIL/Ti₃C₂ composite.*
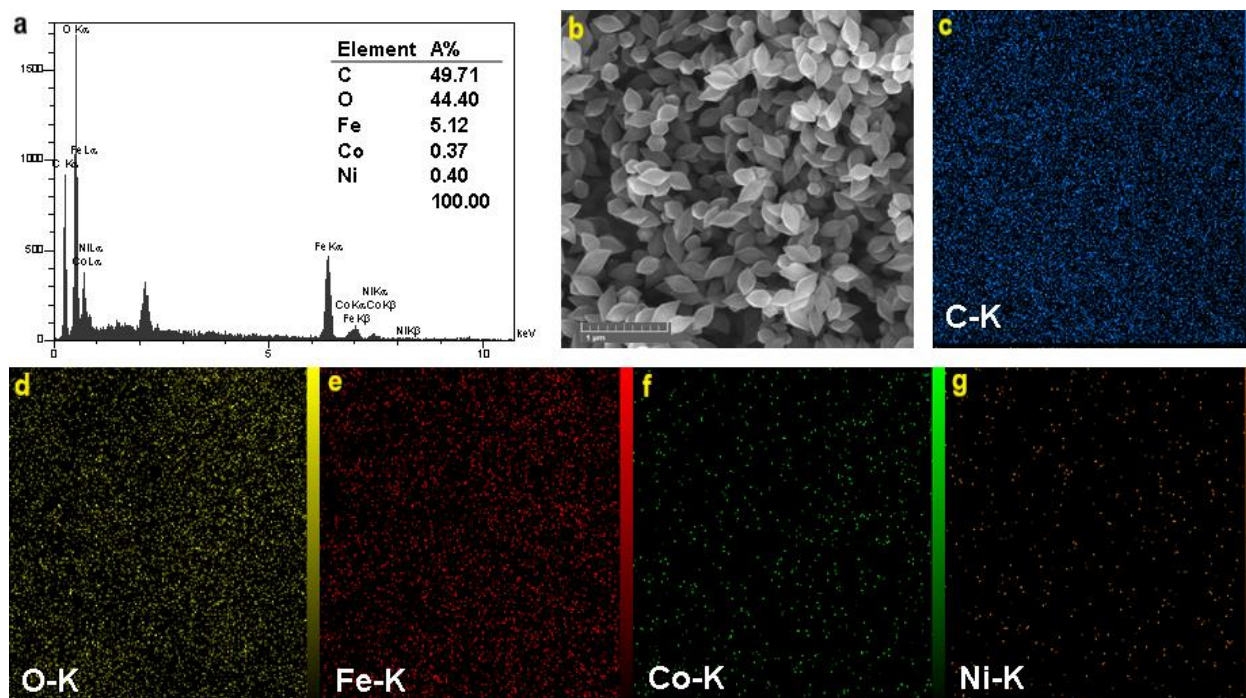

Figure S 3. EDS spectrum and elemental mapping of FeNiCo-MIL. *(a) EDS spectrum of the FeNiCo-MIL, (b) FE-SEM image and (c-g) EDS elemental mappings of carbon, oxygen, iron, cobalt and nickel elements of the FeNiCo-MIL.*
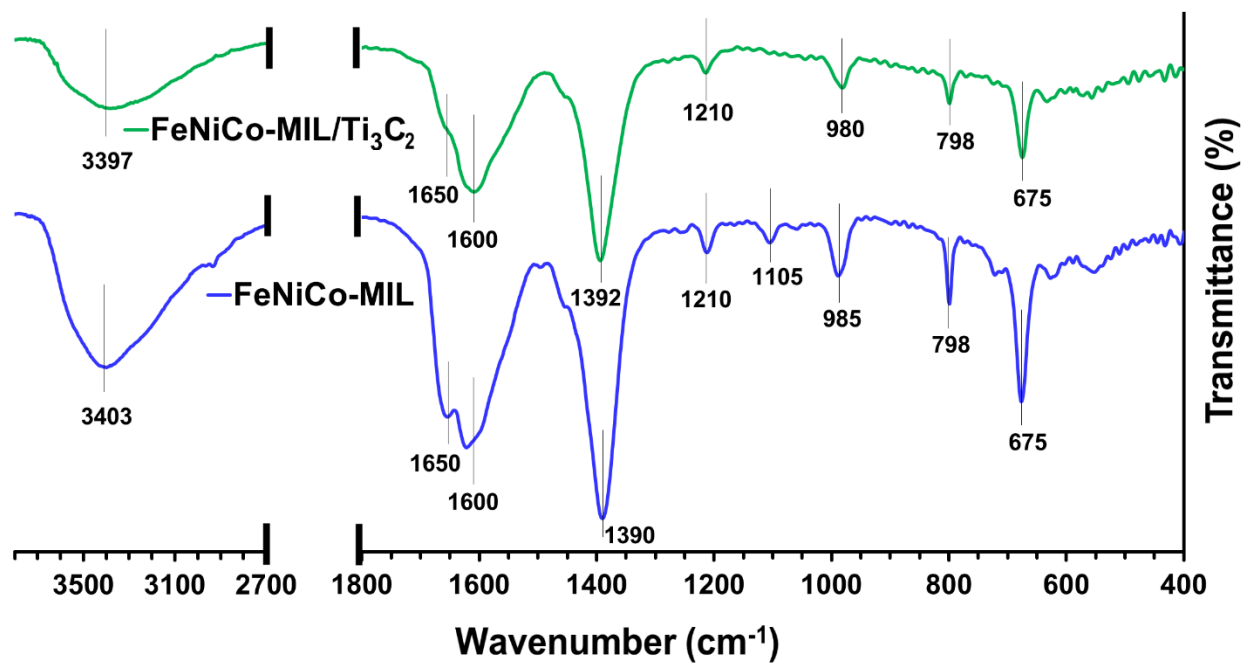
3. FT-IR analysis.

Figure S 4. *FT-IR spectra of the FeNiCo-MIL (blue), and FeNiCo-MIL/Ti$_3$C$_2$ composite(green).*

4. ECSA measurement.

Figure S 5. ***Estimation of the ECSA.*** *CV curves of (a) NF, (b) Ti₃C₂, (c) RuO₂, (d) FeNiCo-MIL, and (e) FeNiCo-MIL/Ti₃C₂, in the non-Faradaic potential window at different scan rates from 20-200 mV s⁻¹ and (f) C_{dl} estimated from the plot of capacitive currents at the middle of the potential window versus scan rate.*

5. Stability investigation of RuO₂ electrocatalyst

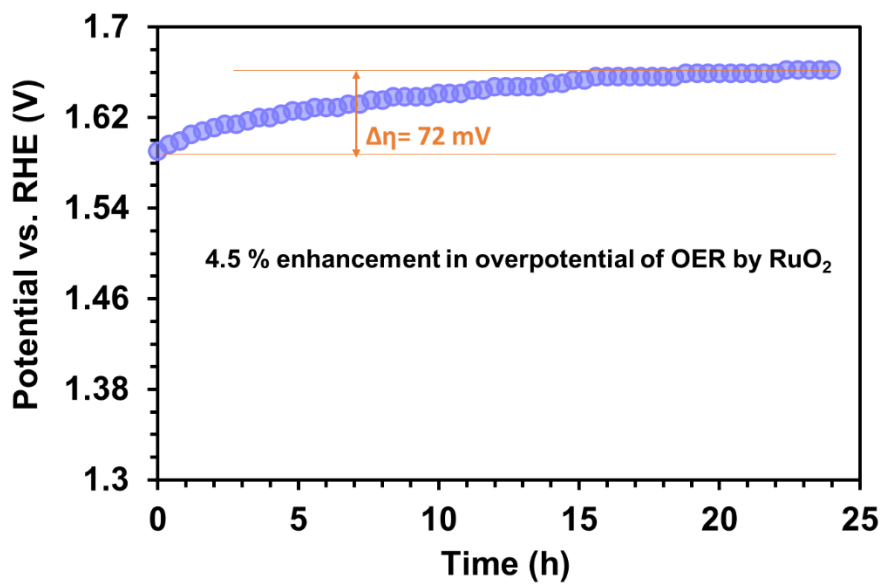*Figure S 6.* Chronopotentiometry plot at the current density of 10 mA cm⁻² for 24 h.

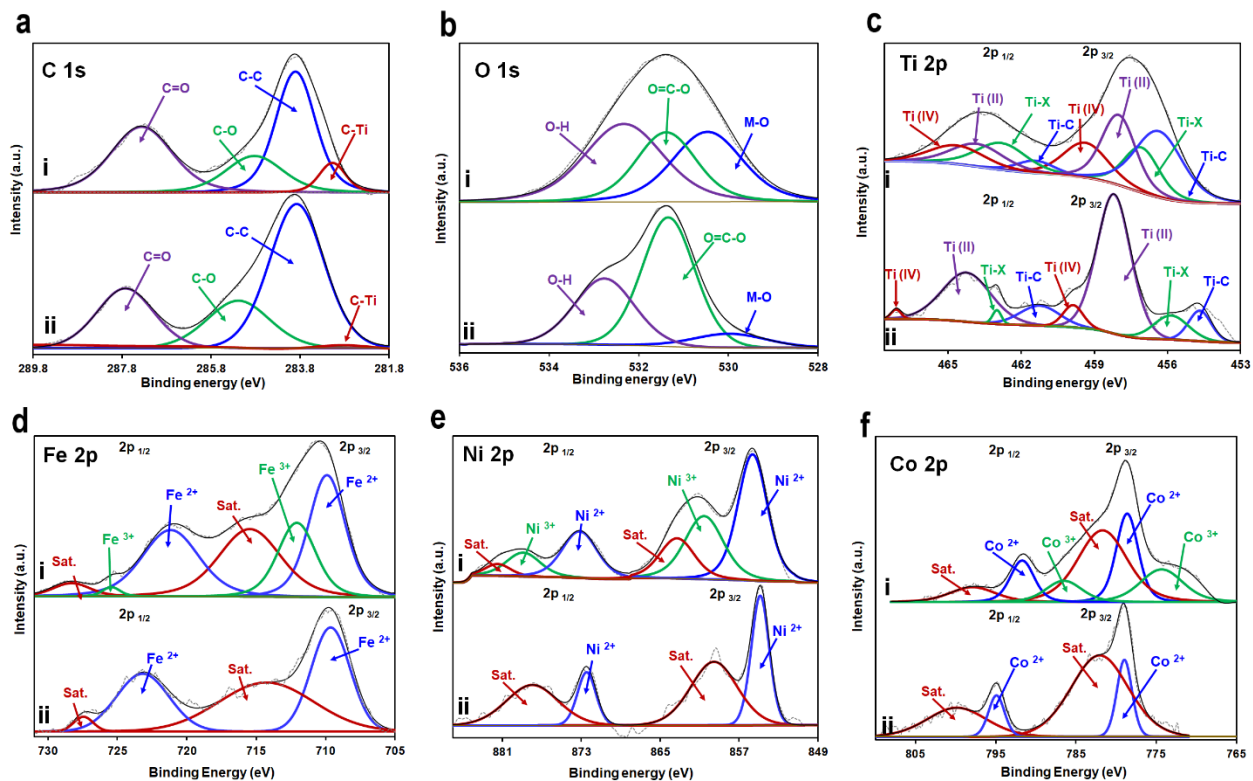## 6. XPS Analysis of FeNiCo-MIL/Ti₃C₂ electrode after stability test.

Figure S 7. *Deconvoluted core-level XPS spectrum of the FeNiCo-MIL/Ti₃C₂ composite, (i) after 24 h chronopotentiometry test at current density of 10 mA cm⁻² and (ii) As-prepared; (a) C 1s, (b) O 1s, (c) Ti 2p, (d) Fe 2p, (e) Ni 2p and (f) Co 2p.*

7. Calculation of the TOF

The surface concentration of metal atoms at the FeNiCo-MIL/Ti_3C_2 electrode was calculated from the redox peak from the LSV.[1]

Area from redox peak of FeNiCo-MIL is $= 13.17 \times 10^{-3}$ Coulombs

Then, no. of electrons $= 13.17 \times 10^{-3}$ C/1.602×10^{-19} C $= 8.85 \times 10^{16}$

Now, divide by the number of e-transferred in the redox reaction which is 1 here.

$= 8.85 \times 10^{16} /1 = 8.85 \times 10^{16}$ atoms

Then TOF calculated as below,

$$TOF = \frac{i \times N_A}{A \times F \times n \times \Gamma}$$

where i is the current (A) at the given overpotential, N_A is the Avogadro number (6.023×10^{23}), A is the geometrical surface area of the electrode (cm^{-2}), F is the Faraday constant (96,485 C mol$^-$^{1}), n is number of electrons and Γ is surface concentration. We have taken the OER current of 37 mA cm^{-2} observed at 1.49 V vs. RHE, and 132 mA cm^{-2} observed at 1.56 V vs. RHE with the loaded catalyst to calculate TOF$_{max}$. Hence we have,

$$TOF_{1.49\ V} = \frac{[(37 \times 10^{-3})(6.023 \times 10^{23})]}{[(1)(96485)(4)(8.85 \times 10^{16})]} = 0.65\ s^{-1}$$

$$TOF_{1.56\ V} = \frac{[(132 \times 10^{-3})(6.023 \times 10^{23})]}{[(1)(96485)(4)(8.85 \times 10^{16})]} = 2.33\ s^{-1}$$

Table S 1. *A comparison of FeNiCO-MIL/Ti₃C₂ electrocatalyst with recently reported catalysts in OER performance.*

Catalyst	Electrolyte	$\eta_{j=10}$ (mV)	Tafel slope (mV dec^{-1})	TOF (s^{-1})	Reference
Ni-BDC/NF	1 M KOH	289	154.5	-	[2]
HZIF-2-CoMo	1 M KOH	277	70	0.01	[3]
$Fe_{2.1}Ni_{0.2}Co_{0.7}$-MIL	1 M KOH	282	51	-	[4]
Fe_2Ni MIL-88	1 M KOH	246	62	-	[5]
$NiSe_2$-FeSe DHPs	1 M KOH	280	58	0.044 @ $\eta_{280\,mV}$	[6]
Fe_xNi_y-BDC	1 M KOH	260	35	0.36 @ $\eta_{330\,mV}$	[7]
$Ti_3C_2T_x$ -CoBDC	0.1 M KOH	410	48.2	-	[8]
CoFe-MOF	1 M KOH	265	44	0.4 @ $\eta_{400\,mV}$	[9]
FeCo-LDH/MXene	1 M KOH	268	85	0.106 @ $\eta_{400\,mV}$	[10]
S-$NiFe_2O_4$@ Ti_3C_2@NF	1 M KOH	270	46.8	-	[11]
NiFeP/MXene	1 M KOH	286	35	0.35 @ $\eta_{300\,mV}$	[12]
Co-B_i/ $Ti_3C_2T_x$	1 M KOH	250	53	-	[13]
Co/N-CNTs@ $Ti_3C_2T_x$	1 M KOH	411	79.1	-	[14]
NiCoFe-HO@NiCo-LDH YSMRs	1 M KOH	278	49.7	0.051 @ $\eta_{278\,mV}$	[15]
S/N-CMF@$Fe_xCo_yNi_{1-x-y}$-MOF	1 M KOH	296	53.5	0.124 @ $\eta_{300\,mV}$	[16]
$NiCo_{2x}Fe_xO_4$ NBs	1 M KOH	274	42	0.016 @ $\eta_{300\,mV}$	[17]
ZnCoFe-N-C	1 M KOH	370	82.9		[18]
FeCoNi-PBA	1 M KOH	236	43.8	0.136 @ $\eta_{320\,mV}$	[19]
t-NiCoFe-LDH	1 M KOH	277	68.83	-	[20]
MXene@RuCo NPs	1 M KOH	253	61.4	0.0113	[21]
NiFeCoP/Mxene	1 M KOH	240	55	-	[22]
CoNi MOF-mCNTs	1 M KOH	306	42	-	[23]
Ru–CoN/$Ti_3C_2T_x$	1 M KOH	290	68	-	[24]
FeOOH NSs/ Ti_3C_2	1 M KOH	400	95	-	[25]
FeNiCo-MIL	1 M KOH	260	42.9	0.71 @ $\eta_{270\,mV}$	This work
FeNiCo-MIL/Ti_3C_2	1 M KOH	231	34.5	2.33 @ $\eta_{270\,mV}$	This work

* Note that, studies shows electrocatalyst activities will always depend greatly on intrinsic activities, therefore TOF is a reliable parameter, but still most researchers employ the overpotential at 10 mA cm^{-2} and Tafel slope parameters which are actually mass dependent and are not very proper criteria for comparison.[26]

Table S 2. *The values of the Equivalent Series Resistance and Charge Transfer Resistance for the FeNiCo-MIL/Ti₃C₂, FeNiCo-MIL and Ti₃C₂ electrodes.*

Catalyst	ESR (Ω)	R_{ct} (Ω)
NF	0.51	29.0
RuO_2	0.34	34.0
Ti_3C_2	0.206	27.5
FeNiCo-MIL	0.404	0.92
FeNiCo-MIL/Ti_3C_2	0.323	0.46

References.

(1) Anantharaj, S.; Karthik, P. E.; Kundu, S. Petal-like hierarchical array of ultrathin Ni(OH)2 nanosheets decorated with Ni(OH)2 nanoburls: a highly efficient OER electrocatalyst. *Catalysis Science & Technology* **2017**, *7* (4), 882-893, 10.1039/C6CY02282K. DOI: 10.1039/c6cy02282k.

(2) Qiang, C.; Liu, M.; Zhang, L.; Chen, Z.; Fang, Z. In Situ Growth of Ni-Based Metal–Organic Framework Nanosheets on Carbon Nanotube Films for Efficient Oxygen Evolution Reaction. *Inorganic Chemistry* **2021**, *60* (5), 3439-3446. DOI: 10.1021/acs.inorgchem.1c00026.

(3) Muthurasu, A.; Dahal, B.; Chhetri, K.; Kim, H. Y. Vertically Aligned Metal–Organic Framework Derived from Sacrificial Cobalt Nanowire Template Interconnected with Nickel Foam Supported Selenite Network as an Integrated 3D Electrode for Overall Water Splitting. *Inorganic Chemistry* **2020**, *59* (6), 3817-3827. DOI: 10.1021/acs.inorgchem.9b03466.

(4) Li, F.; Tian, Y.; Su, S.; Wang, C.; Li, D.-S.; Cai, D.; Zhang, S. Theoretical and experimental exploration of tri-metallic organic frameworks (t-MOFs) for efficient electrocatalytic oxygen evolution reaction. *Applied Catalysis B: Environmental* **2021**, *299*, 120665. DOI: https://doi.org/10.1016/j.apcatb.2021.120665.

(5) Abazari, R.; Sanati, S.; Morsali, A. Mixed Metal Fe2Ni MIL-88B Metal–Organic Frameworks Decorated on Reduced Graphene Oxide as a Robust and Highly Efficient Electrocatalyst for Alkaline Water Oxidation. *Inorganic Chemistry* **2022**, *61* (8), 3396-3405. DOI: 10.1021/acs.inorgchem.1c03216.

(6) Ramesh, S. K.; Ganesan, V.; Kim, J. NiSe2–FeSe Double-Shelled Hollow Polyhedrons as Superior Electrocatalysts for the Oxygen Evolution Reaction. *ACS Applied Energy Materials* **2021**, *4* (11), 12998-13005. DOI: 10.1021/acsaem.1c02634.

(7) Li, J.; Huang, W.; Wang, M.; Xi, S.; Meng, J.; Zhao, K.; Jin, J.; Xu, W.; Wang, Z.; Liu, X.; et al. Low-Crystalline Bimetallic Metal–Organic Framework Electrocatalysts with Rich Active Sites for Oxygen Evolution. *ACS Energy Letters* **2019**, *4* (1), 285-292. DOI: 10.1021/acsenergylett.8b02345.

(8) Zhao, L.; Dong, B.; Li, S.; Zhou, L.; Lai, L.; Wang, Z.; Zhao, S.; Han, M.; Gao, K.; Lu, M.; et al. Interdiffusion Reaction-Assisted Hybridization of Two-Dimensional Metal–Organic Frameworks and Ti3C2Tx Nanosheets for Electrocatalytic Oxygen Evolution. *ACS Nano* **2017**, *11* (6), 5800-5807. DOI: 10.1021/acsnano.7b01409.

(9) Zou, Z.; Wang, T.; Zhao, X.; Jiang, W.-J.; Pan, H.; Gao, D.; Xu, C. Expediting in-Situ Electrochemical Activation of Two-Dimensional Metal–Organic Frameworks for Enhanced OER Intrinsic Activity by Iron Incorporation. *ACS Catalysis* **2019**, *9* (8), 7356-7364. DOI: 10.1021/acscatal.9b00072.

(10) Tian, M.; Jiang, Y.; Tong, H.; Xu, Y.; Xia, L. MXene-Supported FeCo-LDHs as Highly Efficient Catalysts for Enhanced Electrocatalytic Oxygen Evolution Reaction. *ChemNanoMat* **2020**, *6* (1), 154-159. DOI: https://doi.org/10.1002/cnma.201900613.

(11) Tang, Y.; Yang, C.; Yang, Y.; Yin, X.; Que, W.; Zhu, J. Three dimensional hierarchical network structure of S-NiFe2O4 modified few-layer titanium carbides (MXene) flakes on nickel foam as a high efficient electrocatalyst for oxygen evolution. *Electrochimica Acta* **2019**, *296*, 762-770. DOI: https://doi.org/10.1016/j.electacta.2018.11.083.

(12) Chen, J.; Long, Q.; Xiao, K.; Ouyang, T.; Li, N.; Ye, S.; Liu, Z.-Q. Vertically-interlaced NiFeP/MXene electrocatalyst with tunable electronic structure for high-efficiency oxygen evolution reaction. *Science Bulletin* **2021**, *66* (11), 1063-1072. DOI: https://doi.org/10.1016/j.scib.2021.02.033.

(13) Liu, J.; Chen, T.; Juan, P.; Peng, W.; Li, Y.; Zhang, F.; Fan, X. Hierarchical Cobalt Borate/MXenes Hybrid with Extraordinary Electrocatalytic Performance in Oxygen Evolution Reaction. *ChemSusChem* **2018**, *11* (21), 3758-3765. DOI: https://doi.org/10.1002/cssc.201802098.

(14) Zhang, Y.; Jiang, H.; Lin, Y.; Liu, H.; He, Q.; Wu, C.; Duan, T.; Song, L. In Situ Growth of Cobalt Nanoparticles Encapsulated Nitrogen-Doped Carbon Nanotubes among Ti3C2Tx (MXene) Matrix for Oxygen Reduction and Evolution. *Advanced Materials Interfaces* **2018**, *5* (16), 1800392. DOI: https://doi.org/10.1002/admi.201800392.

(15) Niu, Q.; Yang, M.; Luan, D.; Li, N. W.; Yu, L.; Lou, X. W. Construction of Ni-Co-Fe Hydr(oxy)oxide@Ni-Co Layered Double Hydroxide Yolk-Shelled Microrods for Enhanced Oxygen Evolution. *Angewandte Chemie International Edition* **2022**, *61* (49), e202213049. DOI: https://doi.org/10.1002/anie.202213049.

(16) Zhao, Y.; Lu, X. F.; Wu, Z.-P.; Pei, Z.; Luan, D.; Lou, X. W. Supporting Trimetallic Metal-Organic Frameworks on S/N-Doped Carbon Macroporous Fibers for Highly Efficient Electrocatalytic Oxygen Evolution. *Advanced Materials* **2023**, *35* (19), 2207888. DOI: https://doi.org/10.1002/adma.202207888.

(17) Huang, Y.; Zhang, S. L.; Lu, X. F.; Wu, Z.-P.; Luan, D.; Lou, X. W. Trimetallic Spinel NiCo2−xFexO4 Nanoboxes for Highly Efficient Electrocatalytic Oxygen Evolution. *Angewandte Chemie International Edition* **2021**, *60* (21), 11841-11846. DOI: https://doi.org/10.1002/anie.202103058.

(18) Lin, X.; Li, Q.; Hu, Y.; Jin, Z.; Reddy, K. M.; Li, K.; Lin, X.; Ci, L.; Qiu, H.-J. Revealing Atomic Configuration and Synergistic Interaction of Single-Atom-Based Zn-Co-Fe Trimetallic Sites for Enhancing Oxygen Reduction and Evolution Reactions. *Small* **2023**, *19* (30), 2300612. DOI: https://doi.org/10.1002/smll.202300612.

(19) Nguyen, T. X.; Yang, K.-H.; Huang, Y.-J.; Su, Y.-H.; Clemens, O.; Xie, R.-K.; Lin, Y.-J.; Lee, J.-F.; Ting, J.-M. Anodic oxidation-accelerated self-reconstruction of tri-metallic Prussian blue analogue toward robust oxygen evolution reaction performance. *Chemical Engineering Journal* **2023**, 145831.

(20) Karuppasamy, K.; Bose, R.; Velusamy, D. B.; Vikraman, D.; Santhoshkumar, P.; Sivakumar, P.; Alfantazi, A.; Kim, H.-S. Rational Design and Engineering of Metal–Organic Framework-Derived Trimetallic NiCoFe-Layered Double Hydroxides as Efficient Electrocatalysts for Water Oxidation Reaction. *ACS Sustainable Chemistry & Engineering* **2022**, *10* (45), 14693-14704. DOI: 10.1021/acssuschemeng.2c02830.

(21) Li, J.; Hou, C.; Chen, C.; Ma, W.; Li, Q.; Hu, L.; Lv, X.; Dang, J. Collaborative Interface Optimization Strategy Guided Ultrafine RuCo and MXene Heterostructure Electrocatalysts for Efficient Overall Water Splitting. *ACS Nano* **2023**, *17* (11), 10947-10957. DOI: 10.1021/acsnano.3c02956.

(22) Li, N.; Han, J.; Yao, K.; Han, M.; Wang, Z.; Liu, Y.; Liu, L.; Liang, H. Synergistic phosphorized NiFeCo and MXene interaction inspired the formation of high-valence metal sites for efficient oxygen evolution. *Journal of Materials Science & Technology* **2022**, *106*, 90-97. DOI: https://doi.org/10.1016/j.jmst.2021.08.007.

(23) Yu, S.; Wu, Y.; Xue, Q.; Zhu, J.-J.; Zhou, Y. A novel multi-walled carbon nanotube-coupled CoNi MOF composite enhances the oxygen evolution reaction through synergistic effects. *Journal of Materials Chemistry A* **2022**, *10* (9), 4936-4943, 10.1039/D1TA10681C. DOI: 10.1039/D1TA10681C.

(24) Yan, L.; Zhang, B. Rose-like, ruthenium-modified cobalt nitride nanoflowers grown in situ on an MXene matrix for efficient and stable water electrolysis. *Journal of Materials Chemistry A* **2021**, *9* (36), 20758-20765, 10.1039/D1TA05243H. DOI: 10.1039/D1TA05243H.

(25) Zhao, K.; Ma, X.; Lin, S.; Xu, Z.; Li, L. Ambient Growth of Hierarchical FeOOH/MXene as Enhanced Electrocatalyst for Oxygen Evolution Reaction. *ChemistrySelect* **2020**, *5* (6), 1890-1895. DOI: https://doi.org/10.1002/slct.201904506.

(26) Nazari, M.; Ghaemmaghami, M. Approach to Evaluation of Electrocatalytic Water Splitting Parameters, Reflecting Intrinsic Activity: Toward the Right Pathway. *ChemSusChem* **2023**, *16* (11), e202202126. DOI: https://doi.org/10.1002/cssc.202202126.